J Nanostruct 15(4): 1766-1785, Autumn 2025

RESEARCH PAPER

Structural and Functional Investigation of Sodium Alginate-Grafted-Poly (Methacrylic Acid-co-Crotonic Acid)/ Functionalized Single-Walled Carbon Nanotube Hydrogel for Organic Dye Decontamination

Khudhair M. Mahdi [1], Wissam L. Penyan [2], Salam H. Alwan [3] and Layth S. Jasim [4]*

[1] *Department of Chemistry, College of Education, University of Sumer, Thi-Qar, Iraq*

[2] *Ministry of Education, Thi-Qar Education Directorate, Iraq*

[3] *Department of Chemistry, College of Education for Pure Sciences, University of Karbala, Karbala, Iraq*

[4] *Department of Chemistry, College of Education, University of Al-Qadisiyah, Diwaniyah, Iraq*

ARTICLE INFO

Article History:
Received 12 June 2025
Accepted 29 August 2025
Published 01 October 2025

Keywords:
Adsorption isotherm
Hydrogel composite
Kinetic
Safranin-O dye
Thermodynamic

ABSTRACT

polysaccharide through the copolymerization of methacrylic acid (MAA) and crotonic acid (CA) monomers via free-radical grafting in the presence of functionalized single-walled carbon nanotubes (SWCNTs-COOH). The resulting hydrogel composite, designated as SA-g-poly(MAA-co-CA)/ SWCNTs-COOH, was prepared using N,[N′-methylene bis-acrylamide (MBA) as the crosslinker and potassium persulfate (KPS) as the initiator. The primary objective was to develop a novel adsorbent exhibiting enhanced adsorption capacity, superior swelling behavior, and improved reusability for the efficient removal of Safranin-O dye from aqueous solutions. The structural and surface characteristics of the composite, along with its adsorption interactions, were systematically analyzed using FTIR, XRD, FESEM, and TGA. The composite exhibited a point of zero charge (pHpzc) of 3.4 and a swelling capacity of up to 3950% at neutral pH (pH 7). The influence of various operational parameters—including adsorbent dosage, pH, temperature, contact time, and ionic strength—was thoroughly investigated at an initial dye concentration of 200 mg/L. Under optimal conditions (30 °C, pH 7, 0.05 g adsorbent, and 90 min equilibrium time), the hydrogel achieved a maximum removal efficiency of 99.20%. Increasing ionic strength was found to reduce adsorption efficiency. The adsorption process followed the Freundlich isotherm model and was best described by pseudo-second-order kinetics, with the maximum adsorption capacity determined as 366.34 mg/g. Thermodynamic studies indicated that the adsorption was spontaneous and endothermic in nature. Furthermore, the hydrogel composite demonstrated excellent reusability, maintaining an adsorption efficiency above 81.4% after five successive cycles.

How to cite this article
Mahdi K., Penyan W., Alwan S., Jasim L. Structural and Functional Investigation of Sodium Alginate-Grafted-Poly (Methacrylic Acid-co-Crotonic Acid)/Functionalized Single-Walled Carbon Nanotube Hydrogel for Organic Dye Decontamination. J Nanostruct, 2025; 15(4):1766-1785. DOI: 10.22052/JNS.2025.04.025

* *Corresponding Author Email: khudhairmohammed937@gmail.com*

INTRODUCTION

Pollution of the waters is the most important ecological problem since there is a scarcity of drinking water [1]. Water contamination puts both human and other living creatures' health at danger. A recent problem that needs to be handled immediately in order to preserve the planet and its people for future generations is the rapidly growing global contamination of natural resources [2-3]. Among the several forms of organic and inorganic pollutants that are concerning due to their high persistence, capacity to bio accumulate in organisms, and harmful effects on the environment are drugs, organic dyes, steroid hormones, pesticides, and toxic metals [4]. The most widely utilized molecules globally are synthetic dyes [5]. Due to many different kinds of manufacturing processes, the dyes are released into water. examples involve printing purposes coloring fabric, pigmented ink and other related industries. [6]. SF dye may result in negative health outcomes as nasal asthma, allergic reactions, and retinal feeling uncomfortable [7]. Wastewater from these companies, especially in rural locations, is discharged into agricultural fields or aquatic bodies. Safranin-O dyes are utilized for coloring. Consequently, it contaminated agricultural lands and drinking water supplies [8]. Safranin-O dye is nonvolatile and highly dissolves in water. It is a cationic dye of the imine group and has a red hue [9]. It is carcinogenic and hazardous[7]. Flocculation, reverse osmosis, filtering via membranes, photo degradation, biological removal, adsorption, and precipitation with chemicals were the primary techniques used to treat dyes [10]. Although these treatment techniques offer certain options for dye wastewater when compared to adsorption, they also have disadvantages such as low effectiveness, high poisoning of breakdown products, and high cost [11]. The most common of these chemical techniques for treating water is adsorption, which offers benefits including ease of use, high process efficiency, reusability of adsorbent materials, and the absence pollution Hydrogel products are composed of polymer components that have the ability to hold a large amount of water in their three-dimensional natural networks due to their hydrophilic composition [13]. Hydrogels made of natural polymers, such as proteins and polysaccharides that are obtained from plants or animals are essential for encasing pesticides [14]. Sodium alginate and sodium ions can create stable networks for regulated pesticide release [15]. Chitosan, which is formed from chitin, responds to pH changes by expanding and mixing with other polymers to regulate release levels [16-17]. Smart hydrogels, which combine the functionalities of polymers that act as a skeleton to extend the basic functional properties of hydrogels, have recently attracted more attention. These hydrogels have stimuli sensitivity to a variety of environments, including temperature, light, electricity, pressure, CO_2, and pH. This composite hydrogel's different components allow it to exhibit a range of properties [18]. Composite hydrogels are able to perform a variety of tasks by combining different polymers. Several neutral, cationic, and anionic monomers are combined to generate a composite polymer hydrogel [19]. Numerous thorough evaluations of the mechanical and other characteristics of composite hydrogels, as well as their uses, have been published. Hydrogels made from natural polymers have advantages as primary ingredients because of their molecular binding ability, biocompatibility, biodegradability, tenability, and bioactive properties. The hydrogel synthesis uses natural polymers, such as polysaccharides, which are found in nature. Hydrogel can be made from polysaccharides. For example, alginate, collagen, and gelatin have all been used in the production of biomaterials. Natural-source hydrogels are more favorable because polymer hydrogels have been limited in their application for numerous sustainability and safety concerns due to their biodegradability and probable toxicity [20]. nanomaterial's exhibit exceptional physicochemical characteristics, primarily because of their high specific surface area elevated reactivity, which facilitate efficient molecular interactions and improve functional performance. These inherent properties have made it possible for the synthesis of sophisticated nanocomposites through the integration of diverse functional additives. Such additives encompass an extensive variety of inorganic compounds both naturally derived and synthetically produced including clay minerals like silica, bentonite, montmorillonite, and kaolinite [21]. Additionally, carbon-based nanostructures, Particularly, carbon nanotubes with one or more walls (SWCNTs and MWCNTs) are frequently included due to their unique morphology and physicochemical stability [22]. Organic materials, particularly natural polymers, are also employed to further tailor the properties of

the resulting composites. The primary motivation behind the incorporation of these constituents lies in enhancing the adsorption properties of the composite materials. Thanks to their porous nature and complex structural configurations, nanomaterial is capable of strong interactions with a wide array of substances, particularly organic pollutants. This structural advantage leads to improved adsorption performance and increased effectiveness in pollutant removal applications. Carbon nanotubes serve as a prominent example within this class of materials [23]. Their distinctive structural and surface characteristics that make them very efficient.in augmenting the adsorption capacity of composites and participate significantly to the efficient reduction of pollutant from aqueous environments molecules by staking with π–π [24]. In this study, the SA grafted poly (MAA-co-CA-) SWCNTs-COOH acid hydrogel adsorbent shown exceptional adsorption capability and was able to adsorb Safranin O dyes simultaneously. Nevertheless, the adsorption mechanism in this investigation differed from other findings, during adsorption mechanisms. Through the Safranin O dye electrostatic interaction, physical adsorption was achieved. Chemisorption relied on the hydrogel adsorbent's carboxyl, amino, and dye molecules chelating with one another.

MATERIALS AND METHODS

Chemicals

Before to use, neither of the chemicals undergone any more purification, the Sodium alginates. Provided Merck, located in) Darmstadt, Germany (and cheap tubes USA supplied SWCNTs-COOH that has a length of 5–20 um, an outside diameter of less than 8 nm, an internal diameter of 2–5 nm, and a purity > 95%. crotonic acid (AA, 99%) was supplied by CDH Chemical Co. in India. Macklin Biochemical Co., Ltd. provided Methacrylic acid (MAA, 99%). Macklin Biochemical Co., Ltd., Shanghai, China, provided the initiator potassium per sulphate (KPS, 99%) and N, N'-methylene bis-acrylamide (MBA, 99%). The source safranin-O (SF) dye $C_20H_{19}ClN_4$ was Sigma Aldrich Chemical Company. We purchased $CaCl_2$, NaCl, NaOH, and HCl from Merck.

Synthesis of Sodium Alginate Grafted Poly (MAA-co-CA acid)-SWCNT-COOH Hydrogel

A quantity of 0.05 g of carboxyl-functionalized single-walled carbon nanotubes (SWCNTs–COOH) was dispersed in 10 mL of deionized water using ultra sonication for 30 minutes to ensure uniform dispersion. The resulting suspension was then gradually added to a pre-prepared solution of sodium alginate (0.5 g dissolved in 30 mL of deionized water) under continuous stirring. The mixture was subsequently heated to 60 °C under a nitrogen atmosphere to prevent oxidative degradation. following thermal equilibration, 0.7 g of acrylic acid and 0.7 g of methacrylic acid each previously dissolved in 5 mL of deionized water were introduced into the reaction mixture

Fig. 1. Diagrammatic illustration of the synthesis pathway for sodium alginate-g-poly(MAA-co-CA) incorporated with SWCNTs-COOH.

along with 0.05 g of N,N'-methylenebisacrylamide (MBA) as a crosslinking agent. The entire mixture was stirred at ambient temperature for 30 minutes to achieve homogeneity. The prepared solution was then carefully transferred into test tubes and subjected to a water bath at 70 °C for 2 hours to initiate and complete the polymerization process. Upon completion, the former hydrogel composite rods were extracted from the test tubes and sectioned into uniform disc shapes using a sharp-edged blade. To eliminate any unreacted monomers or impurities, the discs were washed in a water–ethanol solution for 30 minutes. The washing solution was replaced periodically until a neutral pH was reached, ensuring the removal of residual contaminants. Finally, the hydrogel discs were thoroughly dried in an oven at 60 °C to obtain the final product. The procedures for preparing hydrogel composites are depicted in Fig. 1.

Characterization

Infrared spectrum employing Fourier transform (FT-IR) was carried out employing Shimadzu instrument (Japan) over the range of frequencies 400–4000 cm^{-1} at a resolution of 8400 s^{-1} to investigate the functional groups present in the hydrogel composite both before and after the adsorption of Safranin-O (SF) dye. This analysis aimed to elucidate the chemical interactions and potential changes in surface functionalities due to the adsorption process. The morphology of surface and microstructural characteristics of the hydrogel composite were investigated using (SEM, MIRA3, Tescan, Czech Republic, Iran) ran at an accelerating voltage of 25 kV, enabling superior resolution imaging of the nanocomposite surface. Crystallinity and phase composition of the hydrogel composite were assessed using X-ray diffraction (XRD) analysis with a Shimadzu XRD-6000 diffract meter (Japan). Cu Kα radiation (λ = 1.5406 Å) was used as the X-ray source, and diffraction patterns were recorded over a 2θ range of 10°–80°, allowing the identification of structural changes induced by composite formation or dye interaction. Thermal stability and decomposition behavior of the synthesized hydrogel composite were evaluated using a thermo gravimetric analyzer (TGA 4000, PerkinElmer), providing insights into the thermal resistance and degradation profile of the material under controlled heating conditions. UV–Vis spectroscopic analysis of the SF dye adsorption process and associated parameters was employed a double-beam UV-Vis spectrophotometer (UV-1800, the Shimadzu company, Japan) for the purpose. This analysis facilitated the monitoring of dye concentration changes and adsorption efficiency under varying experimental conditions.

Swelling Ratio dependence on pH

The pH-responsive behavior of the synthesized hydrogel composite was evaluated through systematic swelling studies. dried hydrogel samples, each with a known weight of 1 g, were immersed in 100 mL Solutions of buffer with varying the pH readings are 1.2, 5.0, 7.4, and 10.0 at ambient temperature to simulate different physiological and environmental conditions. At certain intervals of time, specimens were removed from the swelling media, gently blotted with filter paper to remove surface moisture, and immediately weighed using a precision electronic balance. This procedure was carried out repeatedly until no further weight increase was observed, indicating that the hydrogel had reached its equilibrium swelling state. Equation was utilized to compute the swelling percentage (%).

$$\text{Swelling ratio } (\%) = \frac{W_S - W_d}{W_d} \times 100 \qquad (1)$$

Where: W_d is the dry hydrogel composite's initially weight., W_t is the hydrogel's weight at a specific moment following swelling [25].

Point of Zero Charge (pzc)

The point of zero charge (pHpzc) of the synthesized hydrogel composite was determined using the pH drift method. A series of 150 mL conical flasks were prepared, each containing 50 mL of deionized water. The initial pH values (pHi) of the solutions were adjusted within the range of 2–11 using 0.1 M NaOH and 0.1 M HCl. Subsequently, 0.05 g of the dried hydrogel composite was added to each flask. The suspensions were shaken at 130 rpm for 24 h at ambient temperature to achieve equilibrium. After the contact period, the final pH values (pH_f) were recorded. The difference between the initial and final pH values ($\Delta pH = pH_i - pH_f$) was calculated, and a plot of ΔpH versus pHi was constructed. The point at which ΔpH equals zero was identified as the pHpzc of the composite, representing the neutral surface charge condition

[26].

Adsorption study

At a fixed the starting concentration was 100 $mg.L^{-1}$. Safranine (SF) dye, a systematic optimization of critical adsorption parameters was conducted to elucidate factors governing the adsorption performance of the hydrogel composite. The investigated variables encompassed adsorbent dosage (0.01–0.11 g), adsorption, and contact duration (1–200 min) temperature (10–45 °C), and solution pH (2–10). The pH of the SF dye solutions was precisely adjusted via titration using 0.1 M NaOH and 0.1 M HCl. In each batch adsorption experiment, the hydrogel composite weighed 0.05 g was introduced into 50 mL Flasks made by Erlenmeyer that contain 15 mL of SF dye solution at the predefined initial concentration. The flasks were incubated on a shaker of orbit operating at 130 rpm until the equilibrium of adsorption was reached. Subsequent to the adsorption period, the suspensions were subjected to centrifugation at 5000 rpm for 10 minutes to separate the hydrogel composite from the solution phase. The supernatant's remaining SF dye concentration was quantified by UV–Vis. spectrophotometry at the dye's absorption maximum (λ_{max} = 519 nm). Equations (2) and (3) were used to calculate the equilibrium adsorption capacity (q_e) and adsorption efficiency (R %), respectively. Enabling quantitative evaluation of the hydrogel composite's sorption performance towards SF dye [27].

Adsorption Kinetic

Kinetic analyses provide critical understanding of the rate-determining steps, equilibrium behavior, and overall adsorption dynamics. The experimental findings in this work were interpreted using pseudo-first-order and pseudo-second-order kinetic models. The fictitious initial order model of kinetics, originally developed by Laguerre, is represented by Eq. 2.

$$\ln (q_e - q_t) = \ln\ q_e - K_1 . t \quad (2)$$

Where q_e represents the dye adsorbed quantities upon the hydrogel equilibrium composite in (mg/g), q_t represents the drug adsorbed amounts upon the hydrogel time-composite (mg/g), as well as First-order adsorption rate constant (min^{-1}) is denoted by k_1. The intercept and slope of the linear graph of $\ln(q_e\text{-}q_t)$ and t were utilized to find the computed q_e value, the coefficient of correlation (R^2), and the rate constant of the first order (k_1) as demonstrated in Fig. 7a. The kinetic model of pseudo-second order was applied. For further analyzing the data related to kinetics[28] This model is laid out in Eq. 3:

$$\frac{t}{q_t} = \frac{1}{K_2 . q_e^2} + \frac{1}{q_e} . t \quad (3)$$

The rate constant for second-order adsorption (g/mg min) is represented by k_2, while the amounts of SF dye adsorbed into the hydrogel composite at equilibrium (mg/g) are shown by q_e and k_2 were the equilibrium adsorption values.

Adsorption Isotherm

The isotherms of adsorption of SF dye were investigated in order to clarify the potential for adsorption of hydrogel composite during a variety of temperatures (15, 25, 30, and 35°C), with a dosage of adsorbent 0.05 g, pH of 7, and contact time of 90 min. The amount of adsorbed dye was studied using dye concentrations ranging from 50 to 500 mg/L. At a given concentration, the amount of adsorbed dye increased with a rising primary concentration until equilibrium was reached. To describe the experimental data in the present research, two linear isotherms were used: Langmuir and Freundlich, Fig. 7b represents the outcomes of the experiment. Additionally, (Table 2) offers isotherm parameter values. In accordance Adsorption using a Langmuir isotherm model happens on a single-layer or a fixed amount of adsorption locations, each of which has an equal energy, and the adsorbent structure is assumed to be homogenous. The Langmuir isotherm's linear illustration can be described as follows Eq. 4:

$$\frac{C_e}{q_e} = \frac{1}{q_{max} . K_L} + \left(\frac{1}{q_m}\right) . C_e \quad (4)$$

The adsorbate's equilibrium concentration (mg/L), Langmuir adsorption constant (L/mg), equilibrium adsorption amount (mg/g), and predicted maximum adsorption capacity of the monolayer (mg/g) are represented by the variables C_e, q_e, and K_L. Drawing C_e/q_e vs. C_e will reveal the Langmuir variables, as shown in Fig. 8a.

The Freundlich isotherm clarifies an adsorption mechanism with a heterogeneous surface as well as multilayered structure[29]. Eq. 5 defines the

Freundlich isotherm:

$$\log q_e = \log K_f + \frac{1}{n}\log C_e \quad (5)$$

Freundlich parameters associated with adsorption strength are denoted by n, and The Freundlich adsorption constant (mg/g) is K_f. The intercept and slope were used to determine the K_f and n values, respectively., via plotting $\log q_e$ against log C_e.

Thermodynamic Behavior

By calculating several thermodynamic variables, such as standard change in entropy (ΔS°), standard change in enthalpy (ΔH°), and standard change in free energy (ΔG°), the efficacy of SF dye removal over the hydrogel composite is investigated. Temperatures ranging from 15 to 35°C were used for the experiments. The direction and viability of SF dye adsorption utilizing The hydrogel-based composite was evaluated by means of the thermodynamic coefficients. The thermodynamic coefficients for the adsorption process were determined using the following formulas (Eqs. 6-8) [30].

$$\Delta G^0 = -RT\ln K_d \quad (6)$$

$$\ln K_d = \frac{\Delta S^0}{R} - \frac{\Delta H^0}{RT} \quad (7)$$

$$K_d = \frac{q_e}{C_e} \quad (8)$$

Where T is the operating temperature in Kelvin (K), R is the gas equilibrium constant (8.314 J/mol.K), and K_d is the equilibrium of thermodynamics constant. We will compute the free energy change (ΔG°) using Equation (8). The Van't Hoff plots of $\ln K_d$ vs 1/T (Fig. 9) were used to measure the changes in entropy (ΔS°) and enthalpy (ΔH°). The slop (-ΔH°/R) and intercept (ΔS°/R) [31].

RESULTS AND DISCUSSION

Analysis of FTIR

Before and after dye adsorption, an FTIR study

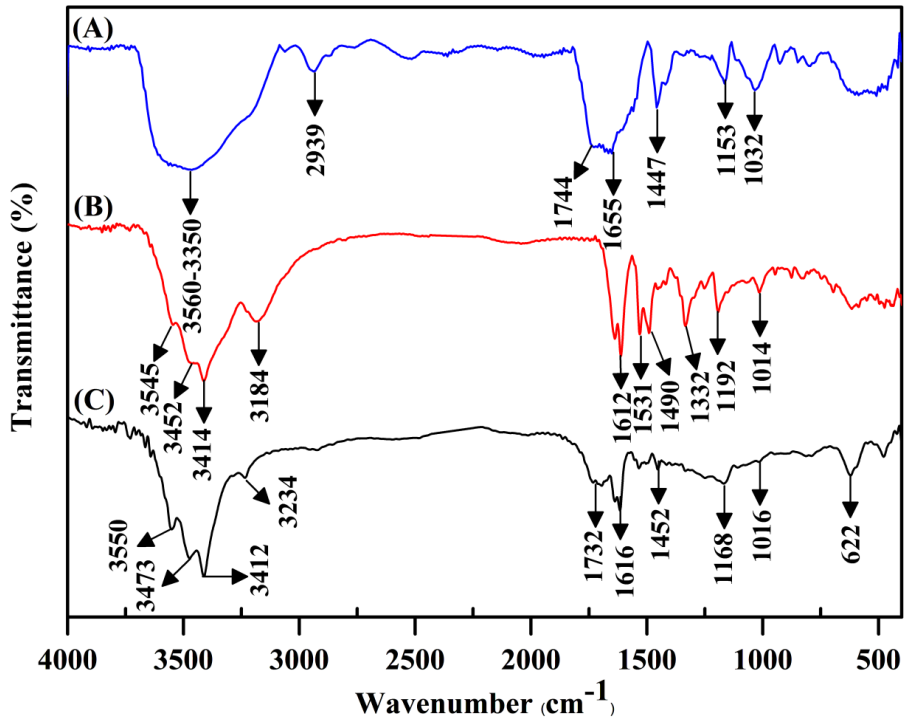

Fig. 2. FTIR spectra of (A) hydrogel composite, (B) SO dye and (C) hydrogel composite After SO dye adsorption.

was performed on the sodium alginate-g-poly (MAA-co-CA) hydrogel weight ratio (1.295%). The study's findings indicated the existence of many different organic functions, with the majority of oxygen, containing functional grouping such OH, COOH, and C-OH. The peak of the broad band of at 3560 cm^{-1}, 3350 cm^{-1}, and 3412cm^{-1} due to the stretching vibrations of the hydroxyl (OH) group. Conversely, peaks in the 2939cm^{-1} region show that -CH_2 asymmetric stretching is present. Additionally, the peaks at 1744cm^{-1}, 1732cm^{-1} correspond to the carbonyl group's (C=O) vibrations of the carboxylic acid group. The peaks in 1665 cm^{-1} due to C=N whereas1612 cm^{-1} due to (C=C) in SF dye. the peaks 1732 cm^{-1} and 1616 cm^{-1} due to C=O and C=C respectively of hydrogel with SF dye indicate take place adsorption [32,33]. The peaks at 1531 cm^{-1}, 1442.40 cm^{-1} and 1412 cm^{-1} certify the presence of carbon-to-carbon (C-C) bending vibrations, while the peaks at 1332 cm-1 indicate the existence of carbon-to-nitrogen (C-N) bond vibrations in SF dye. Additionally, the aromatic rings -OH stretching vibrations were observed at wave numbers 1192cm^{-1}, 1162cm^{-1}, and 1152 cm^{-1}. Additionally, At 1016 cm^{-1} and 1032 cm^{-1}, the tiny peaks represent the aliphatic C-O stretching vibrations. ratio of net hydrogel weight (1.295%) occurs, which is evident from the bands that showed up at 3473 cm^{-1} after dye adsorption. Furthermore, the height and intensity of the bands that first formed at 1732cm^{-1} also changed. The peak in 622 cm^{-1} due to Na-O. In contrast to the C-N band of the raw Sodium alginate-g-poly (MAA-co-CA), which emerged at 1452cm^{-1}, the band at 1447 seemed modest. The adsorption of safranin O dye may involve the hydroxyl, carboxyl, and amine groups. According to these differences in the peaks identified as show Fig. 2 [34-36].

XRD pattern analysis

The x-ray pattern of the generated the hydrogel composite is shown in Fig. 3, and its amorphous nature is evident. due to the absence of any noticeable peaks of diffraction other than a wide band between 2θ =15° and 45°. The XRD Pattern low peaks intensity indicates the hydrogel overlapping with SF dye [37].

FESEM analysis

The surface morphology of the safranin O dye-

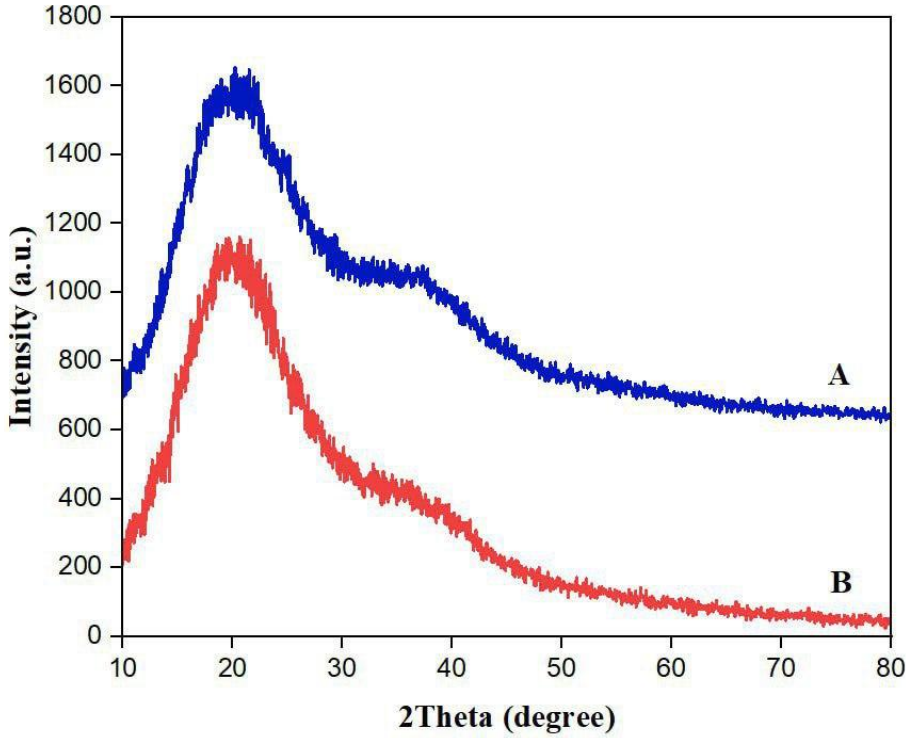

Fig. 3. a- SA-g-poly (MAA-Co-CA) SWCNT-COOH hydrogel composite, b- SA-g-poly(MAA-Co-CA)-SWCNT-COOH hydrogel composite/SF dye.

loaded hydrogel composite, hydrogel composite, and hydrogel composites with safranin O dye was investigated using SEM; the resulting pictures are displayed in Fig. 4a showed particles of hydrogel composite medication that were rougher on the surface and more agglomerated. Prior to SF dye adsorption, A rough, even surface with a few fissures that could serve as solvent entry points for dye loading and swelling was displayed by the hydrogel composite's surface structure. Following SF dye adsorption, the hydrogel composite surface morphology showed a rough, uneven surface with several holes, and the dye particles tended to aggregate. These modifications imply that the SF medication was successfully adsorbed onto the hydrogel composite (Fig. 4b) [38,39].

Analysis of TGA

TGA is an essential technique used to evaluate the polymeric materials' thermal stability by monitoring a sample's weight decrease in relation to temperature (Fig. 5). The curve of TGA of the synthesized hydrogel composite, recorded over a range of temperatures between 40°C and 800 °C, is presented in Fig. 5. The thermal degradation process is characterized by multiple distinct stages of weight loss. The first degradation, occurring 200 °C, is due to the evaporation of moisture content from the composite hydrogel, resulting in a weight loss of approximately 12%. The second degradation stage was noticed 400 °C and is associated, through the breakdown of functional groups like carboxyl (COOH), amine (NH), and carbonyl groups, leading to a weight reduction of 50%. The third stage, extending from 200 to 500 °C, showed a further weight loss of 70%. This stage corresponds to the thermal degradation of the saccharide rings, cleavage of C–O–C linkages within the sodium alginate backbone, degradation of side chains and branches of the grafted copolymer, breakdown of the MAA/CA (methacrylic acid/ citric acid) chains, and decomposition of the cross-linked polymer network. Previous studies have reported that Single-walled carbon nanotubes with carboxyl functionalization (SWCNTs–COOH) exhibit high thermal stability, with minimal mass loss (~2.7%) attributed to the decomposition of surface carboxyl groups within the 100–800 °C range. Therefore, the residual mass following the final decomposition stage is predominantly attributed to the thermally stable SWCNTs. Additionally, the dye-adsorbed polymer composite hydrogel demonstrated enhanced thermal stability compared to the pristine polymer hydrogel. This

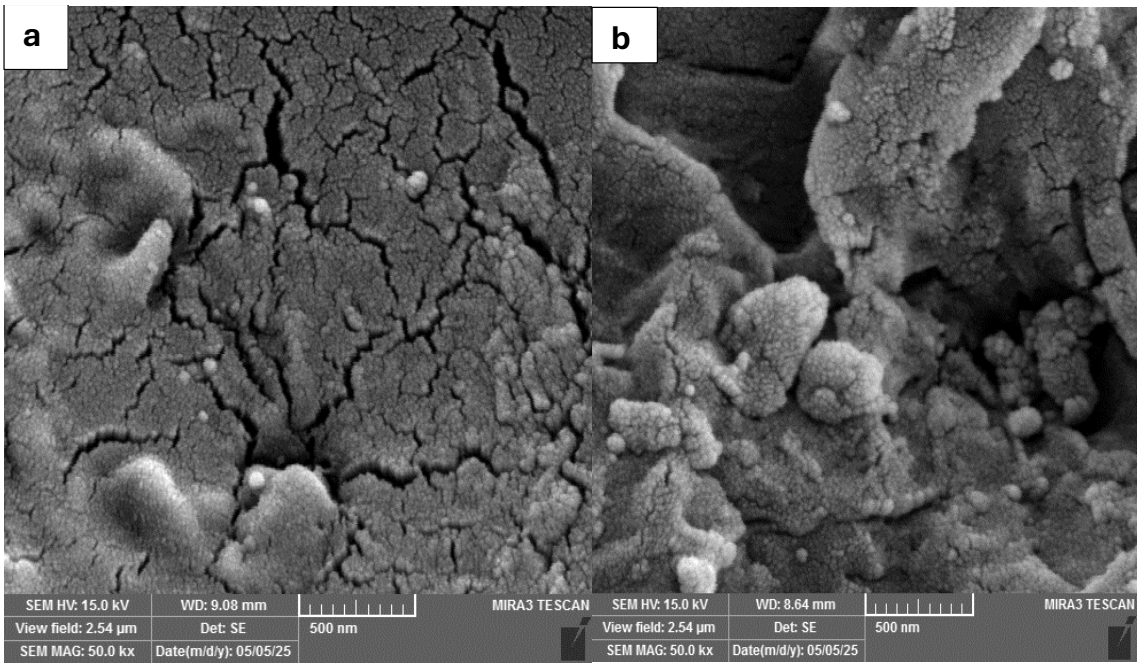

Fig. 4. a- hydrogel composite b- Hydrogel composite packed with SF dye.

increased stability is likely due to the formation of intermolecular interactions between the polymer matrix and dye molecules. As illustrated in Fig. 5b, the total mass loss up to 1000 °C was approximately 85% for the polymer composite hydrogel and 66% for the dye-loaded hydrogel, indicating a significant improvement in thermal resistance upon dye adsorption [40].

Swelling Ratio dependence on pH

The synthetic hydrogel composite's pH-responsive swelling mechanism was systematically evaluated in buffer solutions of varying pH, with the results presented in Figs. 6a and 6b. The hydrogel exhibited significantly enhanced swelling at pH 7.4 and pH 5, while markedly lower swelling ratios were observed at pH 1.2

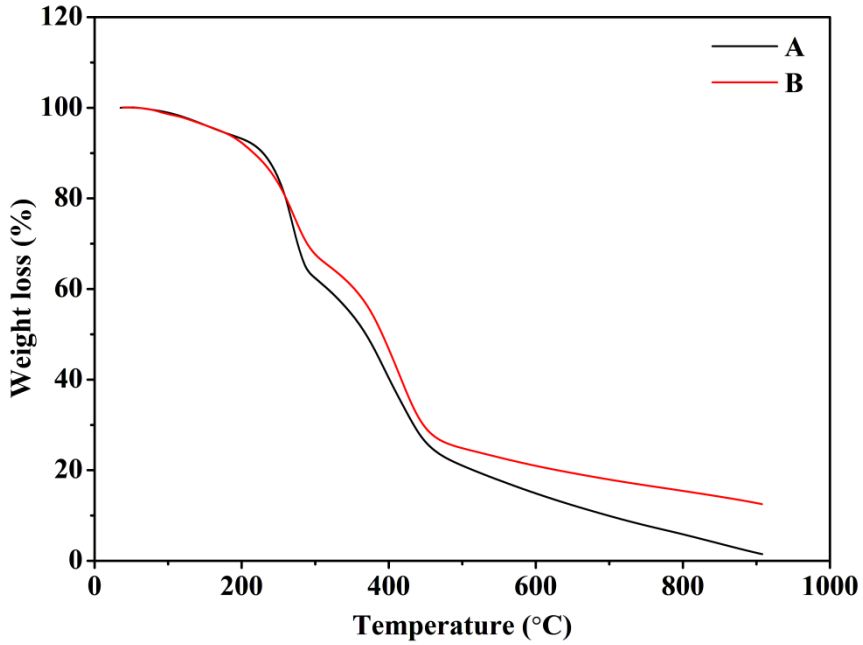

Fig. 5. TGA curves for the hydrogel composite (A) before to SF dye adsorption and (B) after SF dye adsorption.

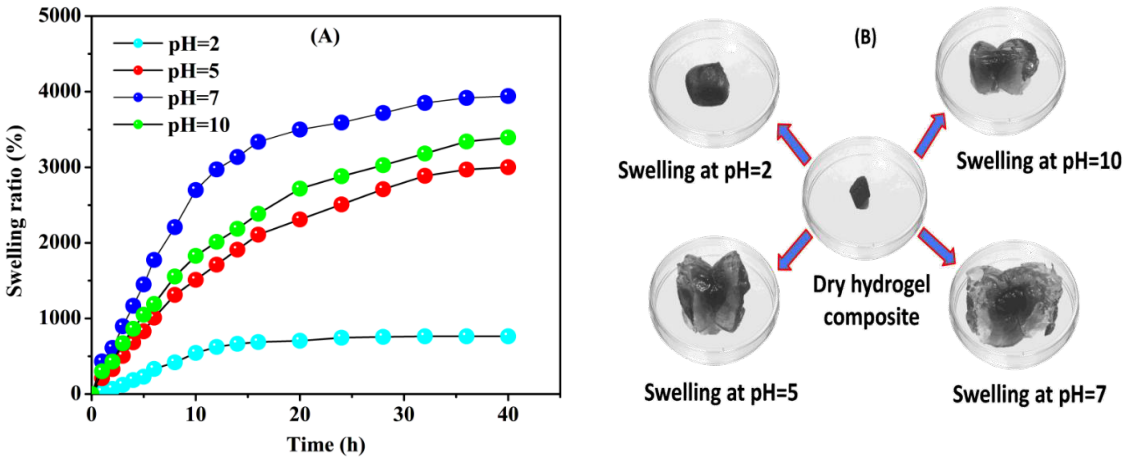

Fig. 6. a- shows how pH affects the hydrogel composite's swelling ratio, b- provides photographic pictures showing how the hydrogel composite swells at various pH levels.

and pH 10, indicating a clear dependence of the hydrogel's swelling properties on the surrounding pH environment. At pH 1.2, the reduced swelling can be ascribed to the carboxylate functional groups' protonation (-COO^-), converting them into carboxylic acid groups **(-**COOH**)**. This protonation disrupts the electrostatic repulsion typically present among negatively charged groups within the polymer network, leading to a collapse of the hydrogel matrix. Furthermore, hydrogen bonding interactions between the protonated carboxylic acid groups contribute to additional network contraction, thereby restricting the ingress of water molecules and diminishing the swelling capacity. Conversely, under physiological pH conditions (pH 7.4), the carboxylic acid moieties undergo ionization to form carboxylate anions (-COO^-). The accumulation of like-charged groups within the hydrogel matrix induces strong electrostatic repulsion**,** resulting in an increase in osmotic pressure. This phenomenon facilitates expansion of the polymer network, promoting enhanced water uptake and a substantial increase in the swelling ratio. At pH 10, the observed reduction in swelling can be ascribed to the counter-ion shielding effect. In alkaline media, the existence of of excess (Na^+) ions leads to the formation of carboxylate salts (-COONa)**,** which neutralize the charges on the polymer chains and significantly reduce electrostatic repulsion. This charge neutralization diminishes the network's ability to expand, thereby inhibiting further swelling, as illustrated in Figs. 6a and 6b [41].

The hydrogel composite's point zero charge

It was found that the hydrogel composite's point of zero charge (pH_{pzc}) was 3.4, as depicted in Fig. 7. This result indicates that at pH values below 3.4, the surface of the hydrogel composite is predominantly positively charged. Conversely, at pH values exceeding the pH_{pzc}, the surface charge transitions to negative, as further illustrated in Fig. 7 [42].

Adsorption condition optimization

The influence of pH on safranin-O dye adsorption onto hydrogel composite

The pH of the solution is a critical parameter influencing adsorption phenomena, as it modulates both the adsorbent and adsorbate species' surface charges, thereby affecting intermolecular interactions and adsorption efficiency. Consequently, pH variations can significantly alter the adsorption behavior of hydrophobic molecules such as Safranin-O (SF) dye. This study examined how pH affected SF's

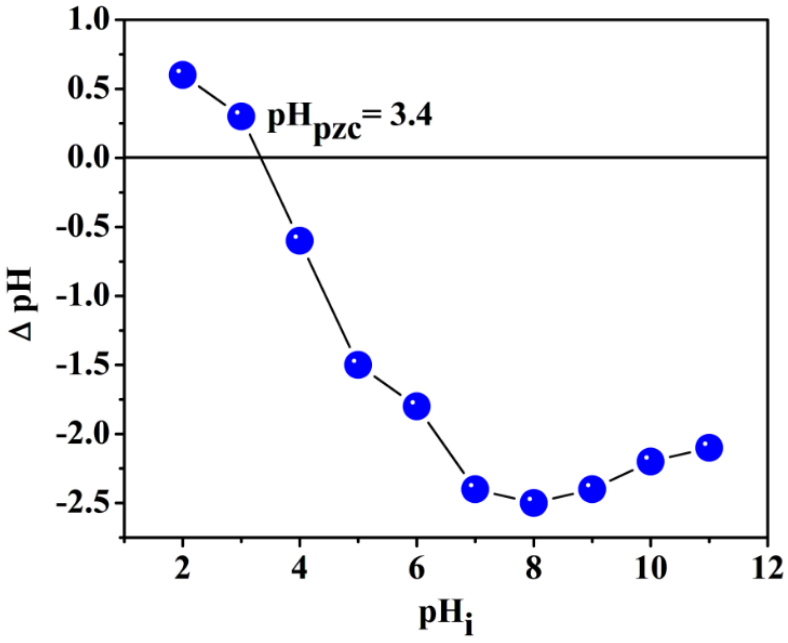

Fig. 7. Point zero charge in a hydrogel composite.

ability to adsorb substances. onto the hydrogel composite was systematically investigated by adjusting the pH of the solution between 3 and 10, while keeping the other experimental parameters constant: 100 mg/L of dye at the beginning, 0.05 g of adsorbent, 90 minutes of contact time, and 40 °C. The results indicate that pH exerts a relatively moderate influence on the adsorption process. Specifically, the removal efficiency of SF increased from approximately 68% at pH 2 to a maximum of 85% at pH 10 (Fig. 8a). Notably, substantial dye uptake (~70%) was observed even at the lowest pH values, reflecting the availability of active adsorption sites on the hydrogel matrix. Adsorption of the cationic SF dye is favored at pH values exceeding. The pH_{pzc} of the hydrogel (3.58) is its point of zero charge, where functional groups such as hydroxyls (-OH) are deprotonated, leading to electrostatic interaction between the positively charged dye molecules and the negatively charged adsorbent sites. In contrast, under highly acidic conditions (pH < pH_{pzc}), the hydrogel surface is positively charged, causing electrostatic repulsion with the cationic SF dye and thus lower adsorption efficiencies. Moreover, the protonation state of the SF dye itself plays a crucial role. The amino group ($-NH_2$) of Safranin-O becomes protonated in acidic media (pKa ≈ 11), which diminishes the capacity for hydrogen bonding interactions with the hydrogel composite[43,44].At elevated pH values, the dye predominantly exists in its deprotonated form, which also reduces the potential for specific interactions between dye molecules and adsorbent surfaces Given this behavior, pH values above 10 were not investigated as dye removal efficiencies are expected to decline beyond this point, consistent with the observed trend in Fig. 8a.

Effect of solution Temperature

The influence of temperature on the adsorption efficiency of Safranin-O dye by the temperature range used to evaluate the hydrogel composite was 15 °C to 50 °C. Results indicate a decline in adsorption capacity as temperature increases [45]. The highest adsorption value, approximately 97.26 mg/g, was recorded at the lowest tested temperature of 15 °C after 90 minutes of contact. At 50 °C, the adsorption capacity decreased slightly to 96.53 mg/g, reflecting a reduction in dye uptake with rising temperature. This trend suggests that lower temperatures favor the adsorption process, likely due to stronger interactions between the dye molecules and the hydrogel matrix at cooler conditions. Furthermore, the capacities measured at 15 °C and 25 °C were nearly identical (97.26 mg/g and 97.09 mg/g, respectively), showing that 25 °C can be considered the optimal temperature for adsorption. The reduction in adsorption capacity at elevated temperatures may be related to changes in the thermodynamic parameters governing [46] the system, where increased thermal energy potentially diminishes the affinity between the adsorbent and adsorbate molecules show as Fig. 8C.

The influence of ionic strength

To investigate the impact of ionic strength on the adsorption capacity (mg/g) for safranin O dye removal using a sodium alginate-g-poly(MAA-co-CA)-SWCNTs-COOH composite, three salts-NaCl, and $CaCl_2$ were introduced at concentrations between 0 and 0.2 g/L. The findings revealed a decrease in adsorption capacity with increasing salt concentrations (Fig. 8e). This trend aligns with observations, noted that elevated ionic strength can diminish dye adsorption due to competition between dye cations and salt cations on the surface of the adsorbent for adsorption sites.Additionally, the compression of the electrical double layer surrounding the adsorbent particles, as reported, further contributes to this reduction in adsorption capacity. Moreover, the presence of divalent metal cations like Ca^{2+} has a more pronounced effect on dye adsorption capacity compared to monovalent cations such as Na^+. For instance, when NaCl concentration increased to 0.2 g/L, the capacity for adsorption for safranin O dye decreased from 39.66 mg/g to 34.45 mg/g. Similarly, the presence of calcium salt ($CaCl_2$) caused a more significant decrease, with the adsorption capacity dropping from 39.66 mg/g to 28.71 mg/these results underscore the importance of considering ionic strength in optimizing conditions for dye removal processes, as higher ionic strengths can impede the adsorption efficiency of composite materials (Fig. 8E) [47-49].

Influence of Contact Time

Concerning removing of dyes from aqueous solutions, the adsorption kinetics of Safranin O dye using sodium alginate-based nanocomposites have been extensively studied. For instance, a study on sodium alginate-g-poly(AA-co-MAA)

SWCNTs-COOH nanocomposite demonstrated that as the contact time increased from 1 minute to 90 minutes, the percentage removal of Safranin O dye rose from 89.70% to 99.18%, with the adsorption capacity (q_e) increasing from 17.94 mg/g to 19.836 mg/g. Beyond 90 minutes, the percentage removal and qe remained relatively constant, indicating the attainment of equilibrium. This trend is consistent with findings from other studies on similar nanocomposites. For example, research on sodium alginate-g-poly (AAM-co-CA) SWCNT-COOH nanocomposite reported that the adsorption capacity and percentage removal of Safranin O dye increased with contact time, reaching equilibrium within approximately 90 minutes. The equilibrium data from these studies were best described by the pseudo-second-order kinetic model, which implies that valence forces are involved through electron sharing or exchange and that the adsorption process is chemisorption-controlled. These findings underscore the importance of contact time in optimizing the

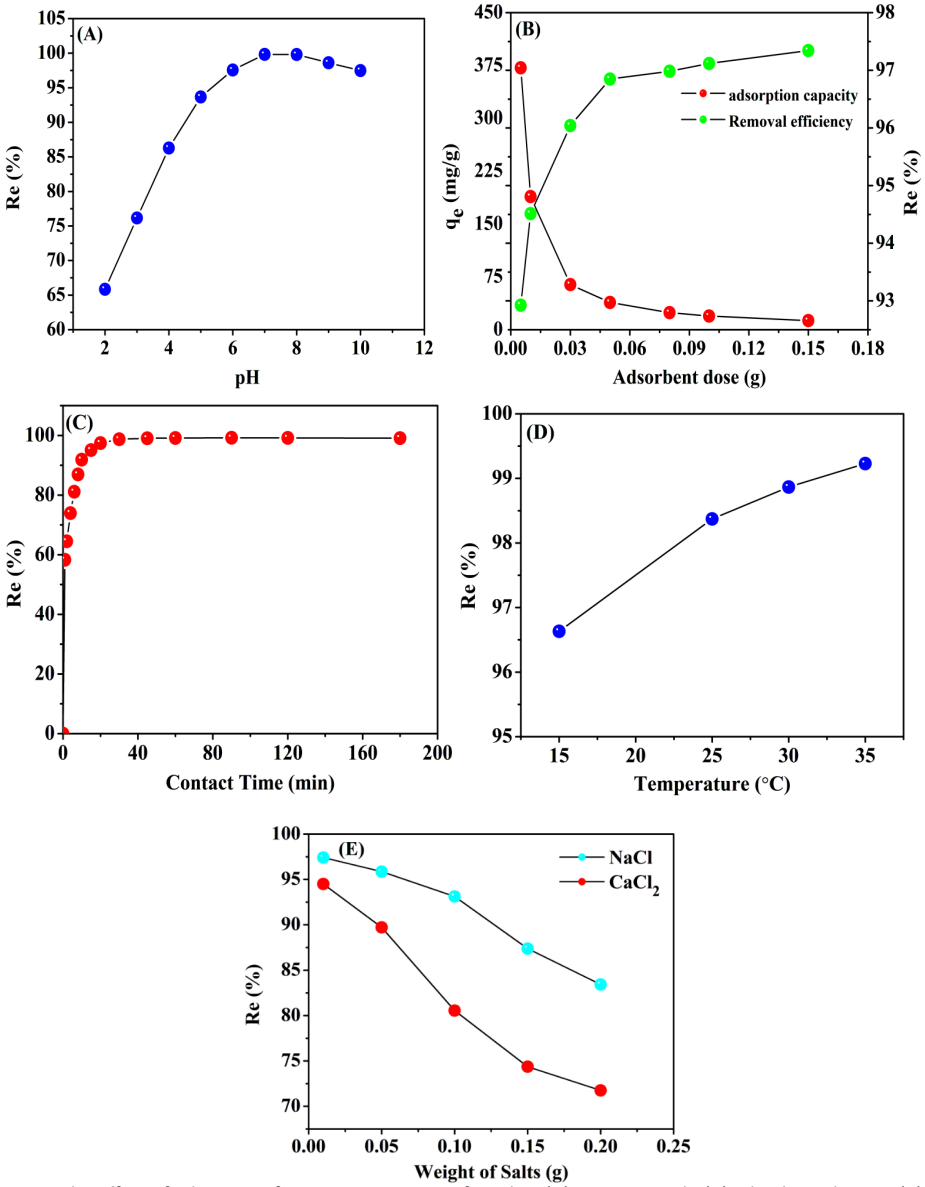

Fig. 8. The effect of adsorption factors on removing of SO dye: (A) ionic strength, (B) adsorbent dosage, (C) contact duration, (D) temperature, and (E) pH.

adsorption process for dye removal. The rapid initial adsorption followed by a slower rate leading to equilibrium suggests that the majority of dye molecules are adsorbed in the early stages, with the remaining sites becoming occupied more slowly. Understanding this kinetics is crucial for designing efficient adsorption systems for wastewater treatment applications [50].

Effect of Concentration of adsorbate

The influence of the initial concentration of Safranin O dye on its adsorption by sodium alginate-g-poly (AAM-co-CA) SWCNTs-COOH nanocomposite was investigated over a concentration 10–500 mg/L in the 308, 318, and 328 K temperature range. Experimental conditions were maintained at pH 4, 0.25 g of adsorbent, and 45 minutes of contact time. According to Fig. 8b, Initially, when the dye concentration rose, the adsorption capability increased, reaching a plateau beyond a certain threshold. This behavior is attributed to the saturation of available active sites on the adsorbent surface, limiting further uptake. The diffusion of dye molecules to the adsorbent surface is improved by increasing dye concentrations because they increase the driving force for mass transfer. Nevertheless, after the active sites are occupied, more dye molecules cannot be adsorbed, leading to stabilization in the uptake capacity. In summary, the adsorption of Safranin O dye by sodium alginate-based nanocomposites exhibits concentration-dependent behavior, with uptake capacity increasing up to a certain concentration before stabilizing due to saturation of the adsorbent surface's active site (Fig. 8C) [51].

Adsorbent dose effect

Optimization of adsorbent dosage is a critical parameter in adsorption studies, as it directly influences both cost-effectiveness and adsorption efficiency. In this work, different amounts of

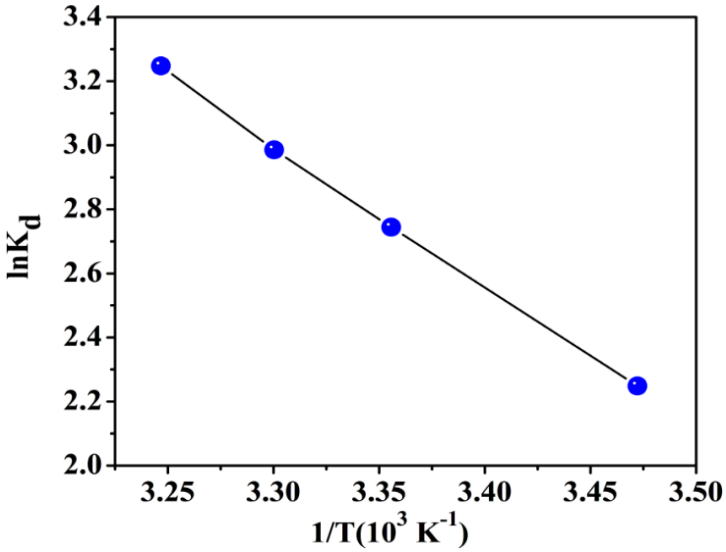

Fig. 9. Thermodynamic models for the adsorption of SF dye onto hydrogel composite.

Table 1. Adsorption of SF dye onto hydrogel composite using thermodynamic parameters.

T(K)	ΔG° (kJ/mol)	ΔH° (kJ/mol)	ΔS° (kJ/K.mol)
287	5.384	36.594	145.697
298	6.799	-	-
303	7.521	-	-
308	8.316	-	-

adsorbent, ranging from 0.005 to 0.15 g, were added separately into 10 mL dye solutions with an initial concentration of 200 mg/L, adjusted to pH 7. The mixtures were stirred continuously for 90 minutes at 35 °C to ensure equilibrium. As presented in Fig. 10, the removal efficiency increased with increasing adsorbent dosage, which can be attributed to the greater availability of active adsorption sites. However, beyond a certain dosage, the removal efficiency reached a plateau, indicating equilibrium despite the presence of additional binding sites. This stabilization may be related to osmotic pressure effects at higher adsorbent levels. Furthermore, the adsorption capacity of Safranin-O dye per unit mass of adsorbent was found to decrease as the dosage increased. This decline can be explained by the aggregation or overlapping of particles, which reduces the effective surface area available for adsorption. Additionally, at higher dosages, the limited number of dye molecules becomes insufficient to occupy all active sites, resulting in reduced dye uptake per unit mass of adsorbent, as illustrated in Fig. 8b [52].

Thermodynamic parameters

The thermodynamic parameters of Safranin-O (SF) adsorption were evaluated using the Van't Hoff equation (Eq. 6, Fig. 9) to determine the changes in entropy (ΔS°) and enthalpy (ΔH°), while the Gibbs free energy change (ΔG°) was calculated accordingly. The calculated thermodynamic values are summarized in Table 1. The results provide several important insights: (i) The positive entropy change (ΔS° ≈ 0.146 kJ/mol·K) suggests an increase in randomness at the solid–liquid interface during SF adsorption. (ii) The positive enthalpy change (ΔH°=36.596 kJ/mol) confirms the endothermic nature of the adsorption process. (iii) The negative Gibbs free energy values (ΔG°) across all studied temperatures demonstrate that the adsorption is spontaneous and thermodynamically favorable. (iv) The increasing adsorption with temperature is further evidenced by higher distribution coefficient

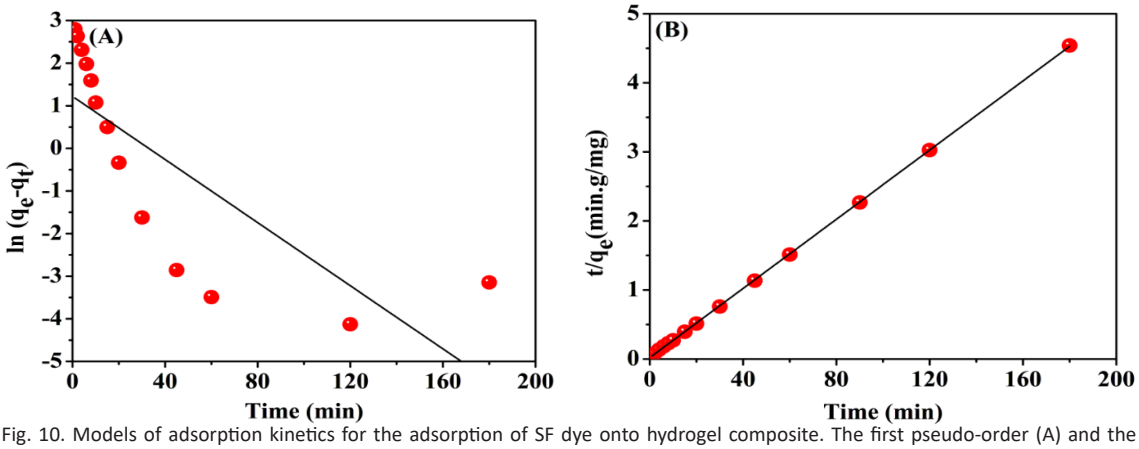

Fig. 10. Models of adsorption kinetics for the adsorption of SF dye onto hydrogel composite. The first pseudo-order (A) and the second pseudo-order (B).

Table 2. Adsorption kinetics of SF dye onto hydrogel composite.

Kinetic models	Parameters	Values
First-order pseudo	$q_{e,\,(exp)}$	39.683
	$q_{e,\,(cal)}$	3.3850
	K_1	0.0370
	R^2	0.5827
Pseudo-second- order	$q_{e,\,(exp)}$	39.683
	$q_{e,\,(cal)}$	39.936
	K_2	0.0299
	R^2	1.0000

(K_d) values and progressively more negative ΔG° values. The magnitude of ΔG° values, ranging from –5.384 to –8.316 kJ/mol, falls within the typical range for physisorption (0 to –20 kJ/mol), whereas chemisorption generally exhibits ΔG° values between –80 and –400 kJ/mol. Similarly, the ΔH° values (22.27–34.54 kJ/mol), being lower than 40 kJ/mol, further support that the adsorption of SF onto the prepared hydrogel-based adsorbents occurs predominantly via physisorption [53,54].

Kinetic Study

To further elucidate the adsorption mechanism, the experimental data were analyzed using the pseudo-first-order, pseudo-second-order, and Elovich kinetic models (Fig. 10 and Table 2). The pseudo-first-order model, commonly applied to heterogeneous adsorption systems, assumes that adsorption occurs through physical interactions, with each active site binding a single adsorbate molecule. In contrast, the pseudo-second-order model attributes the rate-limiting step to chemisorption, where adsorption is governed by chemical interactions between the adsorbent and the adsorbate. The Elovich model also supports chemisorption as the predominant process, describing adsorption on a heterogeneous surface and considering the gradual increase in activation energy over time. The fitting curves of adsorption capacity versus time, illustrated in Fig. 10, confirm the applicability of these models in describing the adsorption behavior [55,56].

Isotherm of Adsorption

The isotherms are illustrated in the graphical representations in Fig. 11, while In Table 3, the isotherm parameters are displayed. Favourable adsorption of the safranin dye onto the hydrogel composite is indicated by a separation factor R value between 0 and 1. The R value was calculated based on different dye concentrations. According to the Model of Freundlich isotherms the value of 1/n is less than one, which suggests that the adsorption process is favorable. Furthermore, as

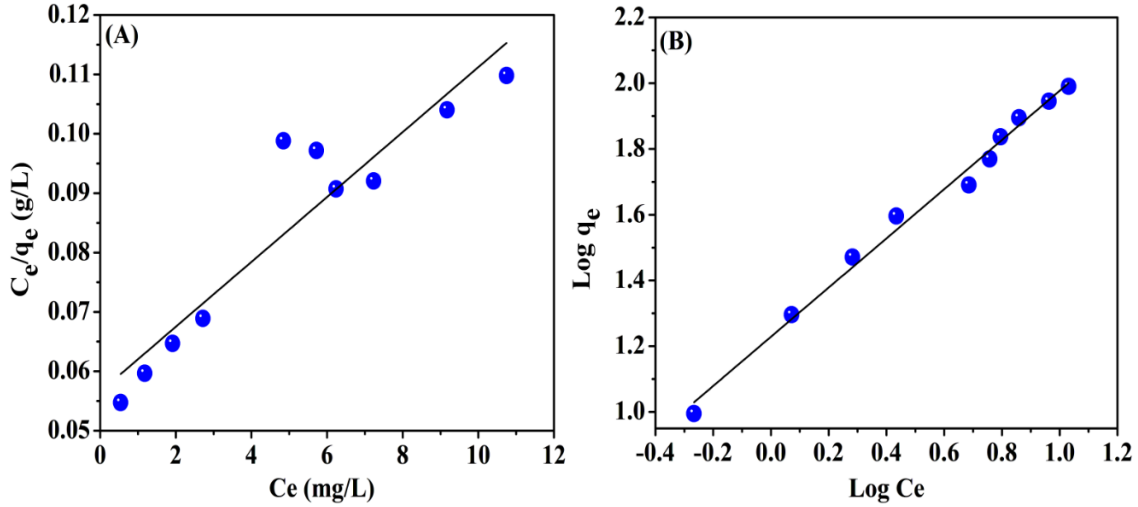

Fig. 11. Adsorption isotherm models for SF dye adsorption onto

Table 3. Isotherm model constants for the hydrogel composite's adsorption of SF dye.

Isotherm models	Parameters	Values
Langmuir	K_L	0.0965
	q_{max}	183.15
	R^2	0.8645
Freundlih	K_F	16.931
	n	1.336
	R^2	0.9909

the temperature rises, the values of the Freundlich constants decrease, indicating that adsorption predominantly occurs at lower temperatures and that the process is fundamentally exothermic. The correlation coefficient R^2 for the Langmuir isotherm is 0.8645, while it is 0.99 for the Freundlich isotherm. This suggests a better fit of the experimental data with the Freundlich model. It is worth noting that The foundation of the Langmuir model is the idea that monolayer adsorption occurs on a uniform surface. Since the Freundlich constant is higher than the Langmuir constant, this further confirms the occurrence of dye adsorption onto the hydrogel's surface composite. Additionally, the value of n in the Freundlich model is greater than one, which implies surface heterogeneity and supports the suitability of the adsorption conditions. This aligns with the multilayer adsorption behavior of the dye on the surface of the hydrogel composite [57, 58].

Regeneration surface

The evaluation of an adsorbent's reusability is a critical factor in assessing its economic feasibility and practical applicability. In this study, deionized water at 60 °C was utilized as the eluent, while hydrochloric acid 0.1M (HCl) served as the regeneration solution during the adsorption-desorption cycles. The hydrogel composite demonstrated exceptional reusability, maintaining over 95% of its initial adsorption capacity after five consecutive cycles [59, 60]. This sustained performance is attributed to the hydrogel's structural integrity and mechanical stability, which are essential for its repeated use in removing both cationic and anionic dyes from contaminated textile wastewater (Fig. 12).

Mechanism of Adsorption

Safranin-O is a cationic dye capable of interacting with the hydrogel composite. The carbonyl oxygen atoms' lone electron pairs within the composite enable binding with the SF molecules. It is expected that electrostatic attractions occur between the positively charged SF dye and the adsorbents negatively charged polar groups. Additionally, weak interactions like π-π stacking and van der Waals forces occur between the hydrogel composite and the aromatic rings of Safranin-O. The potential physical interaction mechanisms include: (1) molecules of dye diffusing into the pores of the composite; (2)

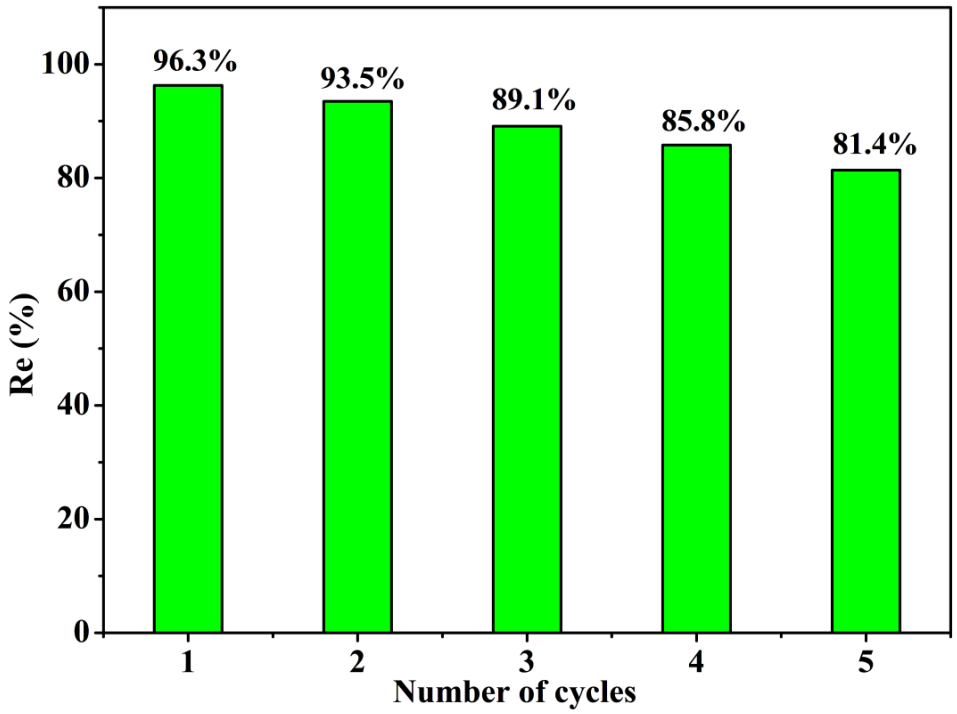

Fig .12. Adsorption–Regeneration Cycles of Hydrogel Composite for SFDye Removal.

hydrogen bonding involving direct carboxyl and hydroxyl group interactions of the composite and the nitrogen atoms in the $-NH_2$ groups of the dye; (3) π-π interactions across aromatic systems; and (4) certain bond-related π-π interactions between the positively charged nitrogen (N^+) in the dye and the aromatic rings of the composite[61,62], as illustrated in Fig. 13.

Comparative Analysis of Safranin-O Adsorption Capacities

The adsorption performance of the synthesized SA-g-poly(MAA-co-CA)/SWCNTs-COOH hydrogel composite was compared with previously reported

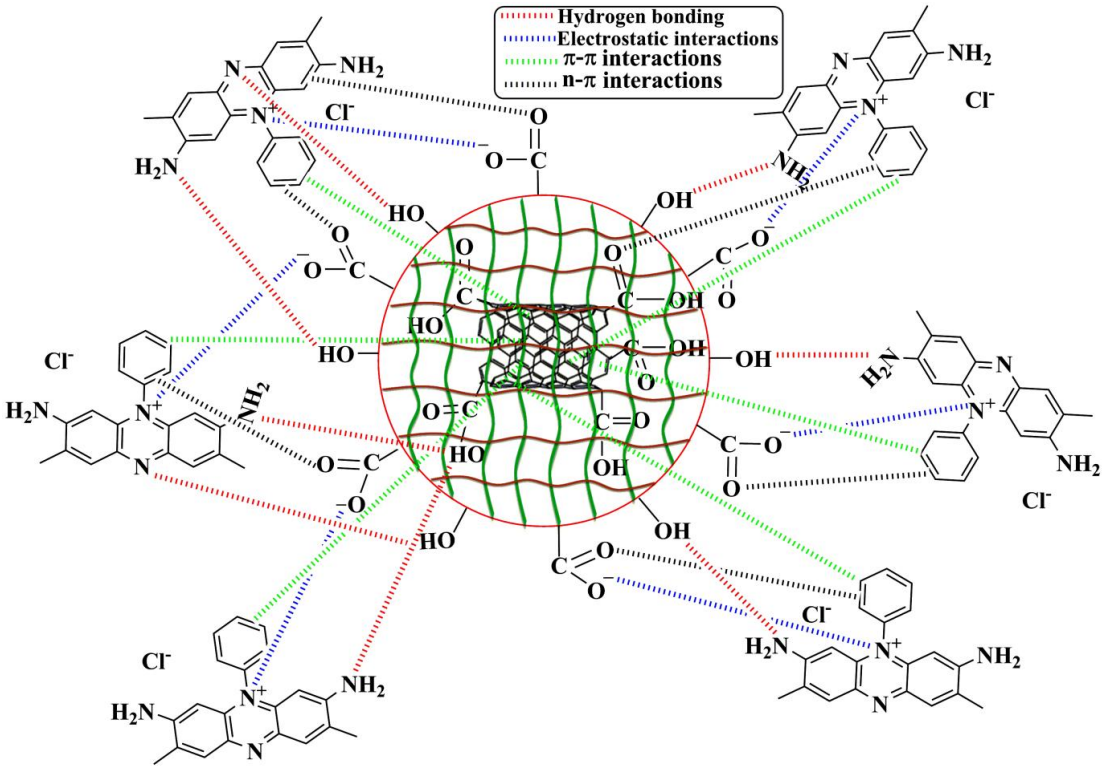

Fig. 13. SF dye and hydrogel composite adsorption mechanisms.

Table 4. Comparing the safranin-O dye's adsorption conditions on various adsorbents.

Adsorbents	Adsorption conditions	q_{max}(mg/g)	References
bentonite/pectin-g-poly(AA-co-CA)	25°C, 120min , pH 7, dose 0.05g	23.115	64
SDS/RM	35°C, 45min , pH 4, dose 0.25g	89.4	65
MSep nanocomposite	25°C, 30min , pH 7, dose 0.07g	18.48	66
MCM-41	30°C, 120min , pH 7, dose 1g	68.8	67
CS-CIT/ZrO_2	25°C, 90min , pH 10, dose 0.05g	280.14	68
Pineapple Peels	20°C, 80min , pH 6, dose 1g	26.08	69
CHI/OP-H_2SO_4	25°C, 59.5min , pH 9.9, dose 0.055g	321.2	70
SA-g-poly(MAA-co-CA)/ SWCNTs-COOH	30°C, 90min , pH 7, dose 0.05g	189.15	This study

adsorbents for Safranin-O removal (Table 4). The maximum adsorption capacity of the present composite reached 189.15 mg/g under neutral conditions (pH 7, 30 °C, 0.05 g adsorbent, 90 min). This value is significantly higher than those obtained with natural or conventional adsorbents such as bentonite/pectin-g-poly(AA-co-CA) (23.115 mg/g), MSep nanocomposite (18.48 mg/g), pineapple peels (26.08 mg/g), and MCM-41 (68.8 mg/g). It also surpassed SDS/RM (89.4 mg/g), highlighting the enhanced adsorption ability imparted by the incorporation of SWCNTs and the synergistic interaction between sodium alginate and the grafted monomers. Although higher adsorption capacities were reported for CHI/OP-H_2SO_4 (321.2 mg/g) and CS-CIT/ZrO_2 (280.14 mg/g), these materials required strongly alkaline conditions (pH ≈ 10) to achieve optimal performance, which may limit their applicability in real wastewater treatment due to the need for pH adjustment. In contrast, the current hydrogel composite exhibits excellent adsorption at neutral pH, which is closer to natural environmental conditions and therefore more practical for large-scale applications. Overall, these findings demonstrate that the developed SA-g-poly(MAA-co-CA)/SWCNTs-COOH hydrogel composite provides a competitive adsorption capacity while maintaining operational feasibility under mild conditions, making it a promising and environmentally sustainable candidate for the removal of cationic dyes from aqueous media (Table 4).

CONCLUSION

The article reports the effective production of a new hydrogel composite reinforced with carboxyl-functionalized single-walled carbon nanotubes (SWCNTs-COOH) based on sodium alginate-grafted poly (methacrylic acid-co-crotonic acid). prepared via free radical copolymerization. The resulting hydrogel composite demonstrated pronounced pH sensitivity, exhibiting maximum swelling behavior at neutral pH (pH = 7). Batch adsorption experiments confirmed the hydrogel's effectiveness in removing Safranin-O SF dye from aqueous solutions. Under optimized conditions 0.05 g of adsorbent, pH 7, a temperature of 35 °C, and an equilibrium time of 90 minutes. A maximum removal capacity of 99.20% was attained by the composite. An ionic strength study revealed that divalent calcium ions ($CaCl_2$) considerably reduced adsorption efficiency compared to monovalent sodium ions (NaCl), highlighting the influence of competing ions. The Freundlich isotherm model provided the best description of the adsorption equilibrium data. while the kinetic behavior followed a pseudo-second-order model, suggesting chemisorption as the rate-controlling step. Thermodynamic analysis indicated that the adsorption process is spontaneous, endothermic, and primarily driven by physisorption. Mechanistic insights suggest that multiple interactions n–π, interactions, π–π stacking, hydrogen bonding, and electrostatic attractions govern the binding of SF dye to the hydrogel composite. Furthermore, regeneration studies demonstrated that the composite retained high performance over five consecutive adsorption–desorption cycles, indicating strong reusability. Overall, this hydrogel composite offers a cost-effective, efficient, and environmentally friendly solution for cationic dye removal, with promising potential for industrial-scale water treatment and environmental sustainability initiatives.

ACKNOWLEDGEMENTS

The authors gratefully acknowledge the University of Al-Qadisiyah, Iraq, for providing the essential facilities and institutional support that enabled the successful completion of this research.

CONFLICT OF INTEREST

The authors declare that there is no conflict of interests regarding the publication of this manuscript.

REFERENCES

1. Sharma S, Bhattacharya A. Drinking water contamination and treatment techniques. Applied Water Science. 2016;7(3):1043-1067.
2. Hofman-Caris R, Hofman J. Limitations of Conventional Drinking Water Technologies in Pollutant Removal. The Handbook of Environmental Chemistry: Springer International Publishing; 2017. p. 21-51.
3. Kundu D, Dutta D, Joseph A, Jana A, Samanta P, Bhakta JN, et al. Safeguarding drinking water: A brief insight on characteristics, treatments and risk assessment of contamination. Environmental Monitoring and Assessment. 2024;196(2).
4. Dehmani Y, Ba Mohammed B, Oukhrib R, Dehbi A, Lamhasni T, Brahmi Y, et al. Adsorption of various inorganic and organic pollutants by natural and synthetic zeolites: A critical review. Arabian Journal of Chemistry. 2024;17(1):105474.
5. Dehmani Y, Dridi D, Dehbi A, Oukhrib R, Adnane I, Lamhasni T, et al. Total Oxidation of Isopropanol in Liquid Phase, Under Atmospheric Pressure and at Low Temperature on a Stable and Inexpensive Catalyst Based on Nickel Oxide Prepared. Chemistry Africa. 2023;7(1):185-193.
6. Amalina F, Razak ASA, Krishnan S, Zularisam AW, Nasrullah

M. Dyes removal from textile wastewater by agricultural waste as an absorbent – A review. Cleaner Waste Systems. 2022;3:100051.
7. Jassim NJ, Younis FH, Alshamkhani MT. Adsorption of Safranin-O Dye Onto Almond Shell Sustainable Activated Carbon: Identifying Key Process Factors and Their Effects. Engineering Reports. 2025;7(1).
8. Bożęcka A, Orlof-Naturalna M, Kopeć M. Methods of Dyes Removal from Aqueous Environment. Journal of Ecological Engineering. 2021;22(9):111-118.
9. Abdul Hussain AF, Halboos MH. Adsorption of safranin dye from their aqueous solutions by using CA and Nano FeO/CA. Journal of Physics: Conference Series. 2020;1660(1):012080.
10. Haleem A, Shafiq A, Chen S-Q, Nazar M. A Comprehensive Review on Adsorption, Photocatalytic and Chemical Degradation of Dyes and Nitro-Compounds over Different Kinds of Porous and Composite Materials. Molecules. 2023;28(3):1081.
11. Cheng J, Wang Z, Cheng X, Wang Z, Wang X. Investigation of the NO removal process of ultra-low temperature adsorption-rapid regeneration. Sep Purif Technol. 2024;330:125522.
12. Pellenz L, de Oliveira CRS, da Silva Júnior AH, da Silva LJS, da Silva L, Ulson de Souza AA, et al. A comprehensive guide for characterization of adsorbent materials. Sep Purif Technol. 2023;305:122435.
13. Kaith BS, Singh A, Sharma AK, Sud D. Hydrogels: Synthesis, Classification, Properties and Potential Applications—A Brief Review. Journal of Polymers and the Environment. 2021;29(12):3827-3841.
14. Zhao L, Zhou Y, Zhang J, Liang H, Chen X, Tan H. Natural Polymer-Based Hydrogels: From Polymer to Biomedical Applications. Pharmaceutics. 2023;15(10):2514.
15. Wang H, Yang L, Yang Y. A review of sodium alginate-based hydrogels: Structure, mechanisms, applications, and perspectives. Int J Biol Macromol. 2025;292:139151.
16. Alsamman MT, Sánchez J. Chitosan- and Alginate-Based Hydrogels for the Adsorption of Anionic and Cationic Dyes from Water. Polymers. 2022;14(8):1498.
17. Lin X, Liu Z, Chen R, Hou Y, Lu R, Li S, et al. A multifunctional polyacrylamide/chitosan hydrogel for dyes adsorption and metal ions detection in water. Int J Biol Macromol. 2023;246:125613.
18. Zhu H, Chen S, Duan H, He J, Luo Y. Removal of anionic and cationic dyes using porous chitosan/carboxymethyl cellulose-PEG hydrogels: Optimization, adsorption kinetics, isotherm and thermodynamics studies. Int J Biol Macromol. 2023;231:123213.
19. El Sayed MM. Production of Polymer Hydrogel Composites and Their Applications. Journal of Polymers and the Environment. 2023;31(7):2855-2879.
20. Mohammed KM, Yousif QA, Habeeb HA. In-situ fabrication a thin-film nanocomposite photo-anode electrode for the dye-sensitized solar cell. Journal of Physics: Conference Series. 2020;1664(1):012092.
21. Khan SA, Khan TA. Clay-hydrogel nanocomposites for adsorptive amputation of environmental contaminants from aqueous phase: A review. Journal of Environmental Chemical Engineering. 2021;9(4):105575.
22. Yousif QA, Mahdi KM, Alshamsi HA. TiO_2/graphene and MWCNT/PEDOT:PSS nanocomposite-based dye-sensitized solar cell: Design, fabrication, characterization, and investigation. Optik. 2020;219:165294.
23. Yousif QA, Mahdi KM, Alshamsi HA. Enhanced photovoltaic performance of dye-sensitized solar cell based on ZnO nanoparticles and ZnO/graphene nanocomposites. J Chin Chem Soc. 2021;68(9):1637-1643.
24. Qin Y, Wei E, Cui C, Xie J. High Tensile, Antibacterial, and Conductive Hydrogel Sensor with Multiple Cross-Linked Networks Based on PVA/Sodium Alginate/Zinc Oxide. ACS Omega. 2024;9(14):16851-16859.
25. El Nemr A, Serag E, El-Maghraby A, Fathy SA, Abdel Hamid FF. Manufacturing of pH sensitive PVA/PVP/MWCNT and PVA/PEG/MWCNT nanocomposites: an approach for significant drug release. Journal of Macromolecular Science, Part A. 2019;56(8):781-793.
26. Mok CF, Ching YC, Osman NAA, Muhamad F, Hai ND, Choo JH, et al. Adsorbents for removal of cationic dye: nanocellulose reinforced biopolymer composites. Journal of Polymer Research. 2020;27(12).
27. Alwan SH, Salem KH, Alshamsi HA. Visible light-driven photocatalytic degradation of Rhodamine B dye onto TiO_2/rGO nanocomposites. Materials Today Communications. 2022;33:104558.
28. Bensalah H, Younssi SA, Ouammou M, Gurlo A, Bekheet MF. Azo dye adsorption on an industrial waste-transformed hydroxyapatite adsorbent: Kinetics, isotherms, mechanism and regeneration studies. Journal of Environmental Chemical Engineering. 2020;8(3):103807.
29. Rigueto CVT, Rosseto M, Nazari MT, Ostwald BEP, Alessandretti I, Manera C, et al. Adsorption of diclofenac sodium by composite beads prepared from tannery wastes-derived gelatin and carbon nanotubes. Journal of Environmental Chemical Engineering. 2021;9(1):105030.
30. Rasoulzadeh H, Mohseni-Bandpei A, Hosseini M, Safari M. Mechanistic investigation of ciprofloxacin recovery by magnetite–imprinted chitosan nanocomposite: Isotherm, kinetic, thermodynamic and reusability studies. Int J Biol Macromol. 2019;133:712-721.
31. Javed T, Khalid N, Javed S, Mirza ML. Adsorptive removal of hazardous cadmium ions from aqueous media using low-rank Pakistani coal. J Dispersion Sci Technol. 2025:1-12.
32. Mohamed F, Abukhadra MR, Shaban M. Removal of safranin dye from water using polypyrrole nanofiber/Zn-Fe layered double hydroxide nanocomposite (Ppy NF/Zn-Fe LDH) of enhanced adsorption and photocatalytic properties. Sci Total Environ. 2018;640-641:352-363.
33. Thakur S, Chaudhary J, Thakur A, Gunduz O, Alsanie WF, Makatsoris C, et al. Highly efficient poly(acrylic acid-co-aniline) grafted itaconic acid hydrogel: Application in water retention and adsorption of rhodamine B dye for a sustainable environment. Chemosphere. 2022;303:134917.
34. Tahermansouri H, Ahi RM, Kiani F. Kinetic, Equilibrium and Isotherm Studies of Cadmium Removal from Aqueous Solutions by Oxidized Multi-Walled Carbon Nanotubes and the Functionalized Ones with Thiosemicarbazide and Their Toxicity Investigations: A Comparison. J Chin Chem Soc. 2014;61(11):1188-1198.
35. Al-Masoudi NA, Mahdi KM, Abdul-Rida NA, Saeed BA, Engel M. A new pregnenolone analogues as privileged scaffolds in inhibition of CYP17 hydroxylase enzyme. Synthesis and in silico molecular docking study. Steroids. 2015;100:52-59.
36. Dai H, Zhang Y, Ma L, Zhang H, Huang H. Synthesis and response of pineapple peel carboxymethyl cellulose-g-poly (acrylic acid-co-acrylamide)/graphene oxide hydrogels. Carbohydr Polym. 2019;215:366-376.
37. Khorasani AC, Shojaosadati SA. Magnetic pectin-Chlorella vulgaris biosorbent for the adsorption of dyes. Journal of Environmental Chemical Engineering. 2019;7(3):103062.
38. Mohan D, Sarswat A, Ok YS, Pittman CU. Organic and inorganic contaminants removal from water with biochar, a renewable, low cost and sustainable adsorbent – A critical review. Bioresour Technol. 2014;160:191-202.
39. Al-Hussainawy MK, Al-Hayder LS. κ-Carrageenan/Sodium Alginate: A New Synthesis Route and Rapid Adsorbent for Hydroxychloroquine Drug. Indonesian Journal of Chemistry.

2023;23(1):219.
40. Patel SR, Patel MP. Green and facile preparation of ultrasonic wave-assisted chitosan-g-poly-(AA/DAMPB)/Fe_3O_4 composite hydrogel for sequestration of reactive black 5 dye. Polym Bull. 2021;79(5):3193-3217.
41. Khater HM, El-Nagar AM. Preparation of sustainable of eco-friendly MWCNT-geopolymer composites with superior sulfate resistance. Advanced Composites and Hybrid Materials. 2020;3(3):375-389.
42. Hasanzadeh M, Simchi A, Shahriyari Far H. Nanoporous composites of activated carbon-metal organic frameworks for organic dye adsorption: Synthesis, adsorption mechanism and kinetics studies. Journal of Industrial and Engineering Chemistry. 2020;81:405-414.
43. Beisenova R, Tulegenova S, Tazitdinova R, Orkeyeva A, Beisenbekova Z. The Problem of Water Resources Pollution with Active Pharmaceutical Substances and the Possibility of Its Solving. Journal of Environmental Management and Tourism. 2022;13(5):1353.
44. Feng S, Liu S, Zhang Z, Feng S, Yuan B, Cheng P, et al. Efficient removal of malachite green dye from aqueous solution using functionalized GO/Fe_3O_4 nanocomposite: kinetic, equilibrium and thermodynamic studies. Desalination and Water Treatment. 2018;109:241-252.
45. Cuerda-Correa EM, Domínguez-Vargas JR, Olivares-Marín FJ, de Heredia JB. On the use of carbon blacks as potential low-cost adsorbents for the removal of non-steroidal anti-inflammatory drugs from river water. J Hazard Mater. 2010;177(1-3):1046-1053.
46. Penyan WL, Jassim IS. Synthesis, characterization and swelling behavior of a novel bio-adsorbent based on pectin grafted poly (acrylic acid -co- itaconic acid) hydrogels for adsorption and controlled release of ciprofloxacin. Springer Science and Business Media LLC; 2024.
47. Yuan Z, Wang J, Wang Y, Liu Q, Zhong Y, Wang Y, et al. Preparation of a poly(acrylic acid) based hydrogel with fast adsorption rate and high adsorption capacity for the removal of cationic dyes. RSC Advances. 2019;9(37):21075-21085.
48. Esmaeli A, Jokar M, Kousha M, Daneshvar E, Zilouei H, Karimi K. Acidic dye wastewater treatment onto a marine macroalga, Nizamuddina zanardini (Phylum: Ochrophyta). Chem Eng J. 2013;217:329-336.
49. Fontana KB, Chaves ES, Sanchez JDS, Watanabe ERLR, Pietrobelli JMTA, Lenzi GG. Textile dye removal from aqueous solutions by malt bagasse: Isotherm, kinetic and thermodynamic studies. Ecotoxicology and Environmental Safety. 2016;124:329-336.
50. Verma A, Thakur S, Mamba G, Prateek, Gupta RK, Thakur P, et al. Graphite modified sodium alginate hydrogel composite for efficient removal of malachite green dye. Int J Biol Macromol. 2020;148:1130-1139.
51. Elsaeed SM, Zaki EG, Omar WAE, Ashraf Soliman A, Attia AM. Guar Gum-Based Hydrogels as Potent Green Polymers for Enhanced Oil Recovery in High-Salinity Reservoirs. ACS Omega. 2021;6(36):23421-23431.
52. Acelas N, Lopera SM, Porras J, Torres-Palma RA. Evaluating the Removal of the Antibiotic Cephalexin from Aqueous Solutions Using an Adsorbent Obtained from Palm Oil Fiber. Molecules. 2021;26(11):3340.
53. Alharby NF, Almutairi RS, Mohamed NA. Adsorption Behavior of Methylene Blue Dye by Novel CrossLinked O-CM-Chitosan Hydrogel in Aqueous Solution: Kinetics, Isotherm and Thermodynamics. Polymers. 2021;13(21):3659.
54. Chafyq EH, Legrouri K, Aghrouch M, Oumam M, Mansouri S, Hassane Khouya E, et al. Adsorption of ciprofloxacin antibiotic on materials prepared from Moroccan oil shales. Chem Phys Lett. 2021;778:138707.
55. Gupta VK, Gupta B, Rastogi A, Agarwal S, Nayak A. Pesticides removal from waste water by activated carbon prepared from waste rubber tire. Water Res. 2011;45(13):4047-4055.
56. Mashkoor F, Nasar A. Magnetized Tectona grandis sawdust as a novel adsorbent: preparation, characterization, and utilization for the removal of methylene blue from aqueous solution. Cellulose. 2020;27(5):2613-2635.
57. Penyan WL, Jasim LS. Preparation and characterization of a novel pH-sensitive pectin-grafted-poly (acrylic acid-co-itaconic acid)/MWCNTs-COOH hydrogel composite for adsorption and controlled release of diclofenac sodium. Carbon Letters. 2024;34(5):1413-1429.
58. Ayouch I, Kassem I, Kassab Z, Barrak I, Barhoun A, Jacquemin J, et al. Crosslinked carboxymethyl cellulose-hydroxyethyl cellulose hydrogel films for adsorption of cadmium and methylene blue from aqueous solutions. Surfaces and Interfaces. 2021;24:101124.
59. Ghzal Q, Javed T, Batool M. Potential of easily prepared low-cost rice husk biochar and burnt clay composite for the removal of methylene blue dye from contaminated water. Environmental Science: Water Research and Technology. 2023;9(11):2925-2941.
60. Batool M, Javed T, Wasim M, Zafar S, Din MI. Exploring the usability of Cedrus deodara sawdust for decontamination of wastewater containing crystal violet dye. Desalination and Water Treatment. 2021;224:433-448.
61. Hussain NA, Jasim LS. Synthesis and characterization of kappa (κ)-carrageenan-grafted poly (acrylic acid-co-itaconic acid)/ multi-walled carbon nanotube (κC-g-poly (AAC-co-IA)/ MWCNT) composite for removing safranin-o dye from aqueous solution. Process Saf Environ Prot. 2025;195:106828.
62. Abbaz A, Arris S, Viscusi G, Ayat A, Aissaoui H, Boumezough Y. Adsorption of Safranin O Dye by Alginate/Pomegranate Peels Beads: Kinetic, Isotherm and Thermodynamic Studies. Gels. 2023;9(11):916.
63. Liu L, Gao ZY, Su XP, Chen X, Jiang L, Yao JM. Adsorption Removal of Dyes from Single and Binary Solutions Using a Cellulose-based Bioadsorbent. ACS Sustainable Chemistry and Engineering. 2015;3(3):432-442.
64. Rafak SH, Jasim LS. Synthesis of novel bentonite/pectin-grafted-poly(crotonic acid-co-acrylic acid) hydrogel nanocomposite for adsorptive removal of safranin O dye from aqueous solution. Int J Environ Anal Chem. 2024:1-24.
65. Sahu MK, Patel RK. Removal of safranin-O dye from aqueous solution using modified red mud: kinetics and equilibrium studies. RSC Advances. 2015;5(96):78491-78501.
66. Fayazi M, Afzali D, Taher MA, Mostafavi A, Gupta VK. Removal of Safranin dye from aqueous solution using magnetic mesoporous clay: Optimization study. J Mol Liq. 2015;212:675-685.
67. Kaur S, Rani S, Mahajan RK, Asif M, Gupta VK. Synthesis and adsorption properties of mesoporous material for the removal of dye safranin: Kinetics, equilibrium, and thermodynamics. Journal of Industrial and Engineering Chemistry. 2015;22:19-27.
68. Abdulhameed AS, Khan MKA, Alshahrani H, Younes MK, Algburi S. Newly developed polymer nanocomposite of chitosan-citrate/ZrO_2 nanoparticles for safranin O dye adsorption: Physiochemical properties and response surface methodology. Materials Chemistry and Physics. 2024;324:129699.
69. Kinetic studies of Safranin-O removal from Aqueous Solutions using Pineapple Peels. Iranica Journal OF Energy and Environment. 2015;6(3).
70. Khan MKA, Abdulhameed AS, Alshahrani H, Algburi S. Development of chitosan biopolymer by chemically modified orange peel for safranin O dye removal: A sustainable adsorbent and adsorption modeling using RSM-BBD. Int J Biol Macromol. 2024;261:129964.